

Optimization of CVD parameters for long ZnO NWs grown on ITO/glass substrate

ABDULQADER D FAISAL

Applied Science Department, University of Technology, Baghdad, Iraq

MS received 12 December 2015; accepted 20 April 2016

Abstract. The optimization of chemical vapour deposition (CVD) parameters for long and vertically aligned (VA) ZnO nanowires (NWs) were investigated. Typical ZnO NWs as a single crystal grown on indium tin oxide (ITO)-coated glass substrate were successfully synthesized. First, the conducted side of ITO-glass substrate was coated with zinc acetate dihydrate to form seed layer of ZnO nanocrystals. Double zone tube furnace connected to vacuum pump was used for ZnO growth process. Zn metal powder was positioned at the first zone at temperature 900°C. The ITO-glass substrate with pre-coated seed layer was then located in the second zone of tube furnace at growth temperature of 550°C. The growth of ZnO NWs was controlled under constant concentration of seed layer, while other parameters such as argon and oxygen flow rates, substrate position, time and oxygen flow rate were varied. The VA ZnO NWs were finally characterized by scanning electron microscopy, X-ray diffractometer and high-resolution transmission electron microscope equipped with energy-dispersive X-ray spectroscopy. The results show that long and VA ZnO NWs were single crystalline with hexagonal wurtzite structure. The ultimate length and average diameter of ZnO NWs were 10 μm and 50–100 nm, respectively. These were achieved under optimized CVD growth parameters. The mechanism of vertical growth model of ZnO NWs is also discussed.

Keywords. VA ZnO NWs; chemical vapour deposition; long ZnO nanowires; ZnO single crystal; growth mechanism.

1. Introduction

Zinc oxide (ZnO) is a II–VI compound semiconductor with a wide direct energy bandgap of 3.37 eV and high exciton binding energy of about 60 meV at room temperature [1,2]. ZnO as nanostructures have been found useful in many applications such as optoelectronics [3], photovoltaic [4], gas sensors [5], dye-sensitized solar cells [6,7], catalytic activity [8] and photo catalytic activity [9]. Several methods have been reported for the synthesis of various ZnO nanostructures, such as hydrothermal [10], sonochemical [11,12], sol-gel [13–15] and microwave irradiation [16]. Although conventional methods such as chemical vapour deposition (CVD) [17,18], vapour solid (V–S) [19], vapour trapping CVD [20], vapour phase transport deposition [21], electron beam evaporation [22] and thermal oxidation [23] can produce various ZnO micro or nanostructures, they often suffer from problems of high temperature, need for high vacuum, lack of control and high cost. It is crucial to have a controlled morphology of the nanostructures for the desired applications. Many different morphological ZnO nanostructures have been fabricated, including nanowires (NWs) [24], nanorods (NRs) [25,26], nanobelts [27], nanoflowers [28], nanospheres [29], nanorings [30], nanoribbon [31] and nanosaw [32]. In the present work, synthesis of long and vertically aligned (VA)

ZnO NWs on indium tin oxide (ITO)-glass substrate was conducted with the optimization of CVD growth parameters.

2. Experimental

2.1 ITO-glass substrate cleaning

The ITO substrate cleaning is one of the conventional methods used to remove surface contaminants and to provide a clean ITO surface to enhance the adhesion of seed layer onto its substrates. So, the ITO-glass substrate was cleaned prior to the seed layer preparation. Pieces of ITO-coated glass (1.0 × 1.0 cm²) substrates were gently washed with detergent solution and deionized (DI) water subsequently, then each of them were sonicated with acetone and isopropyl alcohol for 30 min and washed with DI water. Finally, they were dried under a stream of pure nitrogen and backed on hot plate at 150°C for 5 min.

2.2 Preparation of ZnO seeds layer

The growth of ZnO NWs begun firstly with ZnO seed layers coating as nanocrystals. The seed layer solution was always prepared by dissolving 0.015 M of zinc acetate dihydrate [Zn(CH₃COO)₂·2H₂O] in 10 ml of ethanol (CH₃OH) and then sonicated for 30 min. Later it was cooled down at room temperature to make it ready for use. The conductive side of

abdulf330@gmail.com

ITO-glass substrate ($1 \times 1 \text{ cm}^2$) seed layer was coated by drop casting method using $20 \mu\text{m}$ pipette. This layer was left for 20 s to interact with the surface. The ITO-glass with seed layer was rinsed with ethanol for few seconds and then followed by drying with a stream of N_2 gas. The previous steps were repeated four times to insure having enough thickness of ZnO seed layer on the substrate. The seed layers coated on ITO-glass substrate became ready for loading into the quartz tube for simultaneous baking and growth processes.

2.3 Growth parameters for ZnO NWs on ITO-glass

There are several CVD growth parameters of the ZnO NWs, which can be investigated in the present work. These parameters need to be selected properly during the growth of ZnO NWs on ITO-glass. The growth of the ZnO NWs were controlled under constant concentration of seed layer, while other parameters such as argon and oxygen flow rates, substrate position, time and oxygen flow rate were varied. The source temperature selection mainly depends on the volatility of the source material (Zn powder). The substrate temperatures determine the morphology of ZnO nanostructure that will be grown on it.

2.4 Growth process of ZnO NWs on ITO-glass

The ZnO NWs to be investigated in this article were synthesized by vapour-solid (VS) process. In principle, thermal evaporation technique is a simple process in which condensed or powder source material is vapourized at elevating temperature, then the resultant vapour phase is condensed under certain parameters mentioned previously (section 2.3) to form the desired product. The growth processes are carried out in a horizontal three zone tube furnace (SWGL-1600X/MTI Corp.) as shown in schematic diagram of figure 1, which is composed of a horizontal tube furnace with

quartz tube (3 cm diameter and 120 cm long), rotary pump system and digital mass flow metres control system, through which gases are supplied. The right-hand end of the quartz tube is connected to the rotary pump. Both ends are sealed with rubber O-rings (Viton) through stainless-steel screw connectors. The ultimate vacuum pressure for this configuration is $\sim 2 \times 10^{-3}$ Torr, measured by Edward vacuum gauge connected to a digital vacuum controller. The carrier gas is introduced from the left end of the quartz tube and is pumped out at the right end. The source material is a very fine pure Zn powder (Alfa Aesar Supplier), loaded on an alumina boat and positioned at the highest temperature region of the quartz tube. The pre-cleaned ITO-glass substrates were placed at a distance downstream for collecting growth products. This simple set-up can achieve high control of the final product.

2.5 Characterization techniques

The crystal structures of ZnO films were characterized by X-ray diffractometer (Pan analytical Thin film/small-angle X-ray diffraction (SAXS)) with $\text{CuK}\alpha$ ($\lambda = 0.1546 \text{ nm}$) radiation. The surface morphologies of the ZnO films were observed by scanning electron microscope (SEM/JEOL-JSM 5140) equipped with energy dispersive X-ray spectrometer (EDX). High-resolution transmission electron microscope, TEM JEOL-2000 EX, 200 kV, equipped with EDX was used to analyse the ZnO nanostructures.

3. Results and discussion

The main purpose of this investigation is to find the optimum CVD parameters to grow VA with long, small diameter and high-density ZnO NWs on ITO-coated glass. These parameters can simply be obtained by varying the flow rate of argon and oxygen gases, the position of the substrates and the growth time. The growth experiments were conducted at

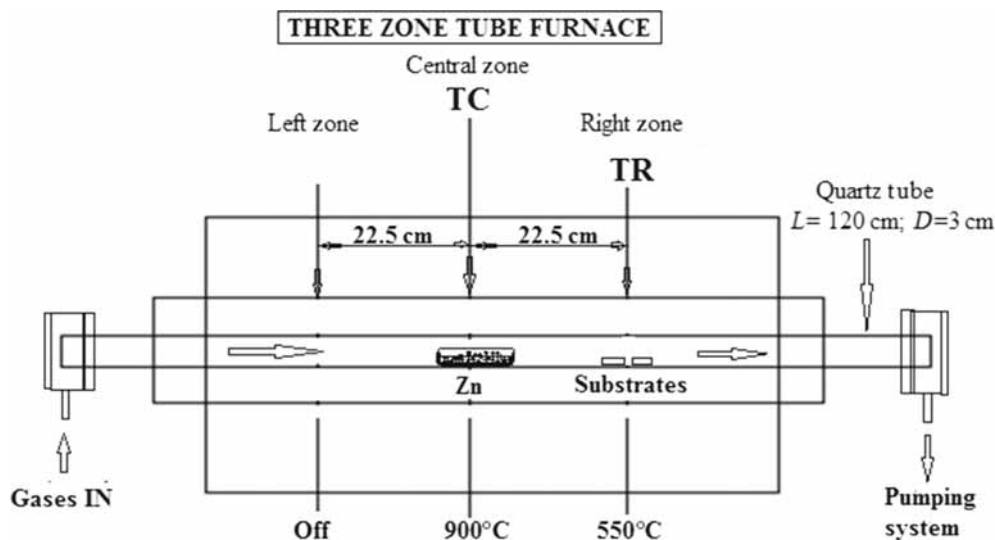


Figure 1. Schematic diagram of the experimental apparatus for growth of oxide nanostructures by the solid-vapour phase process.

constant value of ZnO seed layer concentration. The central and right zone temperatures of the tube furnace were kept constants during the experiments. The growth of ZnO NWs as a function of argon and oxygen flow rates, substrate position, time and oxygen flow rate variations was investigated.

3.1 Growth of ZnO NWs as a function of Ar and O₂ gases variation

The first group of investigation was carried out to study the growth ZnO NWs by varying the flow rates of Ar and O₂ gases at fixed ratios of Ar/O₂, 100/10, 200/20 and 300/30, under the following fixed conditions: weight of Zn powder is 2 g, furnace temperature at the centre TC = 900°C and at the right side TR = 550°C (figure 1), reaction time 20 min, and

the final growth pressure of 100 Torr. Figures 2–4 show the SEM images of as-synthesized ZnO NWs under various flow rates of argon to oxygen gases. The SEM results show that long, VA and high-density ZnO NWs with different diameters have been synthesized. The average length of ZnO NWs was measured to be about 5 μm at various flow rates of Ar and O₂ (100/10, 200/20 and 300/30), while the average diameters of the wires decreased from 200 to 40 nm for S1 and from 120 to 25 nm for S2, respectively, as explained in table 1. Two conclusions have to be mentioned here, the first one is that the variation in gases flow rates have no effect on the length of the wire. The second one is related to decreasing of wire diameters, which is due to the temperature decreasing of samples position of S1 to S2. So, it could be ruled that sample position at lower temperature has smaller diameter

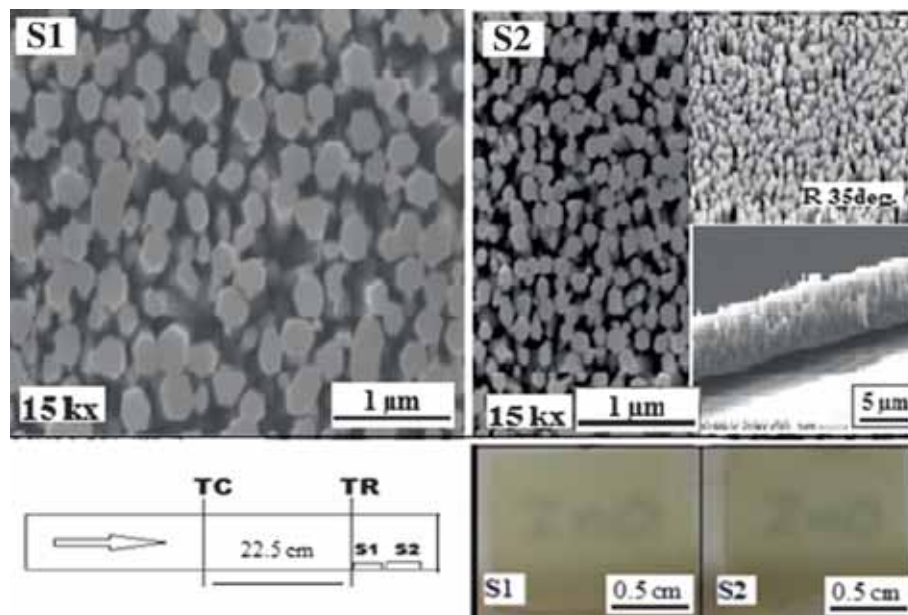


Figure 2. SEM images for ZnO NWs growth on ITO-glass at argon to oxygen = 100/10 sccm for 20 min at 550°C.

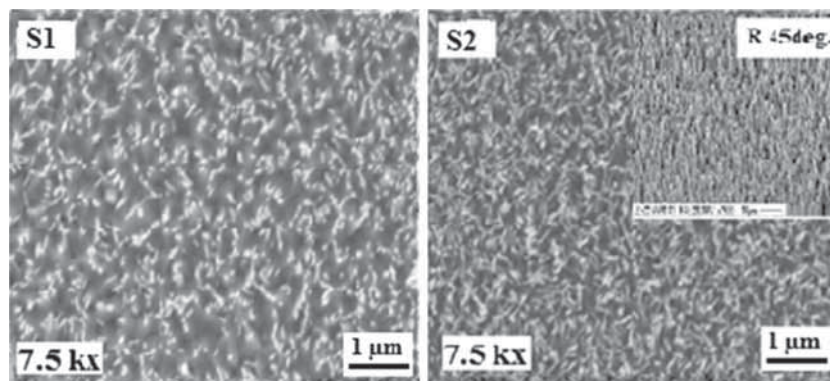


Figure 3. SEM images of ZnO NWs growth on ITO-glass at argon to oxygen flow rate = 200/20 sccm for 20 min at 550°C.

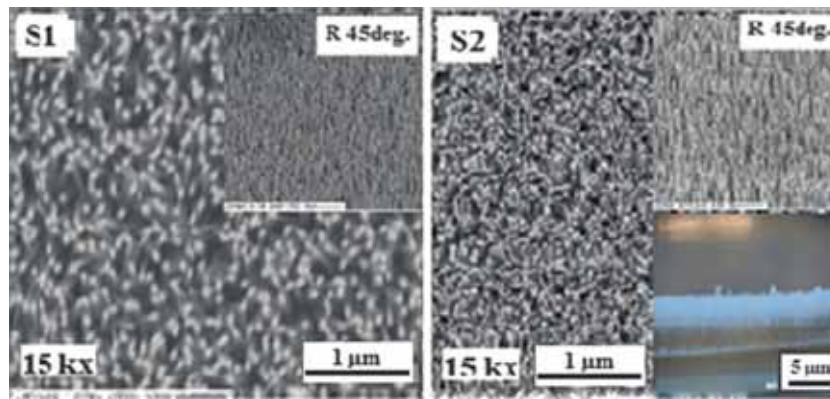


Figure 4. SEM images of ZnO NWs growth on ITO-glass at argon to oxygen flow rate = 300/30 sccm for 20 min at 550°C.

Table 1. Morphology measurements of ZnO NWs grown on ITO-glass substrate at various Ar and O₂ flow rates.

Exptl. code no.	Ar/O ₂	ZnO NWs length (μm)	Average diameter of S1 (nm)	Average diameter of S2 (nm)	Aspect ratio L/D	SEM morphology
CVD 24/Fig. 2	100/10	5	200	120	25	Wires with hexagonal C.S
CVD 26/Fig. 3	200/20	—	80	40	—	Wires with tipped ends
CVD 25/Fig. 4	300/30	5	40	25	200	Wires with circular C.S

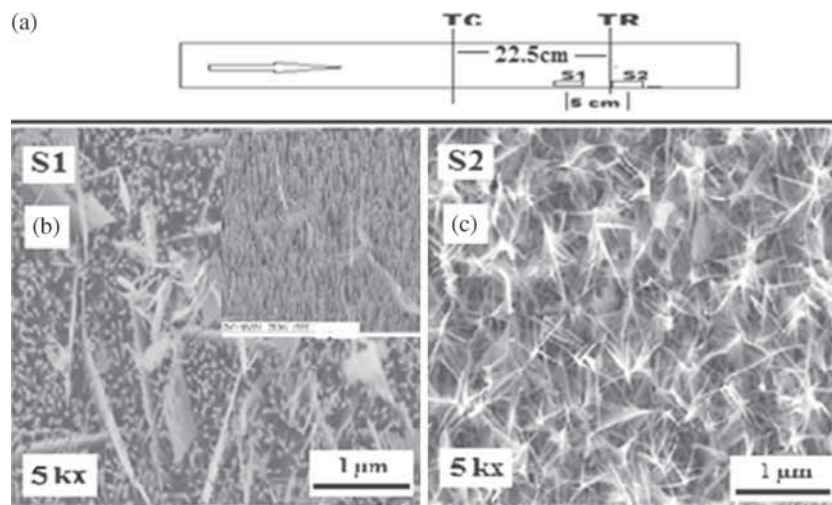


Figure 5. SEM images of ZnO NWs growth on ITO-glass; (a) sketch of substrate position, (b) S1: high density of VA ZnO NWs and comb-like nanostructures; and (c) S2: high density of ZnO NWs and fish bone-like nanostructures.

and vice versa. This could be due to the seed layer grain size variation as a function of temperature and large grains with high temperature and vice versa. The lengthy and VA NWs are shown in the insets of figures 2 and 4. High aspect ratio (L/D) can be obtained from 25 to 200. The NWs shown in figure 2 for S1 sample are all separated and have different diameters and the top ZnO NWs are clearly flat with

hexagonal shape. This confirms that nonanalytic growth with cleaned surface were synthesized. So, no metal catalyst was used to grow VA ZnO NW arrays. This suggested VS model to grow these NW arrays. Figure 2 shows an optical micrograph of typical ZnO NWs grown on ITO-glass with semi-transparent and yellowish colour. Moreover, the major benefit of this investigation is to offer the possibility of

growing ZnO NWs at short growth time of 20 min and higher at the indicated parameters. Hence, increase in the growth time could be reflected on the length of the NWs.

3.2 Growth as a function of substrate position variation

The second group of investigation was carried out to study the substrate position influences on the morphology of ZnO nanostructures growth. The substrate positions can be regarded as temperature variation relative to the source materials position. So, higher temperature was obtained when the substrates were closer to the source material and vice versa. This could be mostly affected by the morphology of the nanostructures growth. In addition, the vertical growth mode is also investigated relative to the substrate position and their mechanism will be discussed later. Figure 5 shows SEM images for two samples (S1 and S2) corresponding to the positions of the samples explained in figure 5a. SEM images in figure 5b demonstrates the growth of sample S1 positioned at a distance of 18 cm from TC, which shows a very small VA ZnO NWs as a first layer (VA ZnO NWs at the inset on top corner) and low-density comb-like nanostructure grown on the top of the NWs. Figure 5c also shows another ZnO fish-like bone nanostructure. This study proves that different substrate positions results in different morphologies

of ZnO nanostructures. The present result is different compared with the previous investigation explained in section 3.1.

The main reason for these different morphologies is the saturation vapour pressures of Zn. This is varied with respect to the substrate positions.

3.3 Growth of ZnO NWs as a function of time variation

The third group of investigation was carried out to study the time variation under constant Ar to O₂ flow rates of 300 to 30 sccm, respectively. The growth of ZnO NWs was conducted at central zone temperature of 900°C and right zone temperature of 550°C at reaction times of 20, 40 and 60 min, respectively. The substrate position was kept at 22.5 cm from the source material location (Zn powder at TC) as explained in figure 1. Figures 6 and 7 show the SEM images, which revealed the effect of growth time on the morphology of ZnO nanostructures. The dependence of NWs average length on the reaction time is shown in figure 8. The length of NWs increased slightly when the growth time increased from 20 to 60 min. The ZnO NWs synthesized at 20, 40 and 60 min have lengths of 5, 5 and 7 μm, respectively (figure 8). Compared to those grown for a shorter time, the average diameter did not change significantly, indicating that the growth

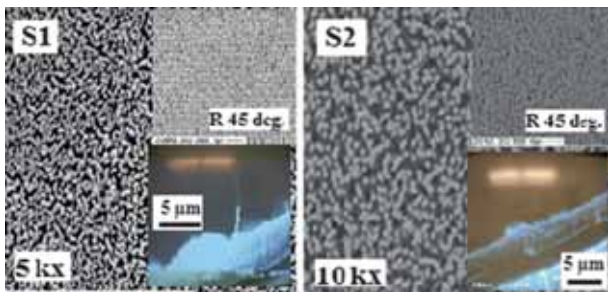


Figure 6. SEM images of ZnO NWs growth on ITO-glass/40 min 15 mM, Zn = 3 g (insets represent images at 45° and cross-sections).

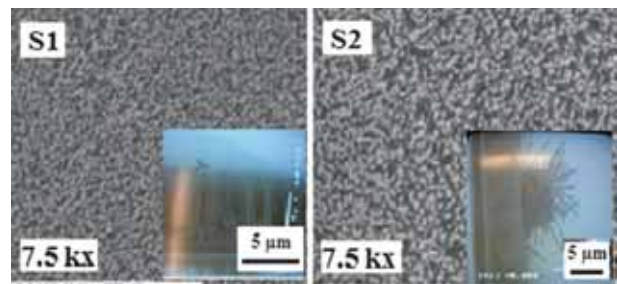


Figure 7. SEM images of ZnO NWs growth on ITO-glass/60 min 15 mM, Zn = 4 g (insets represent cross-sections).

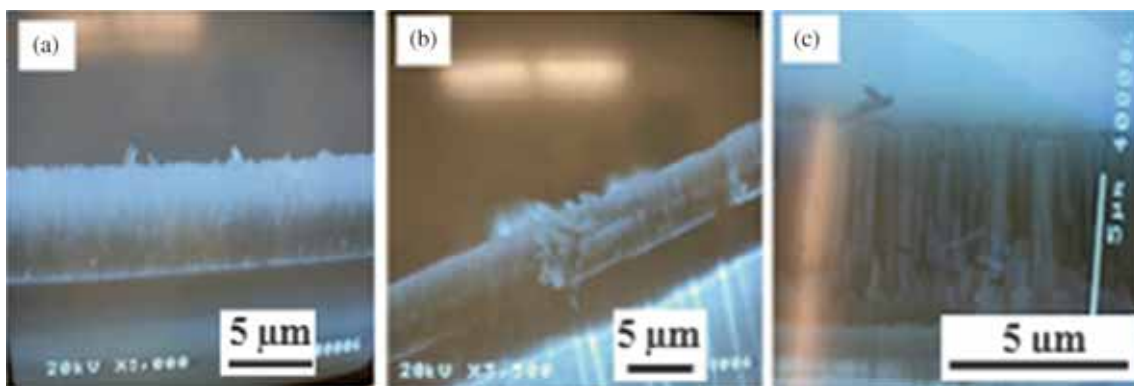


Figure 8. SEM cross-sectional images of ZnO NWs growth on ITO-glass with wire lengths of (a) 5, (b) 5, (c) 7 μm, at various growth times 20, 40 and 60 min, respectively. Ar/O₂ = 300/30 sccm.

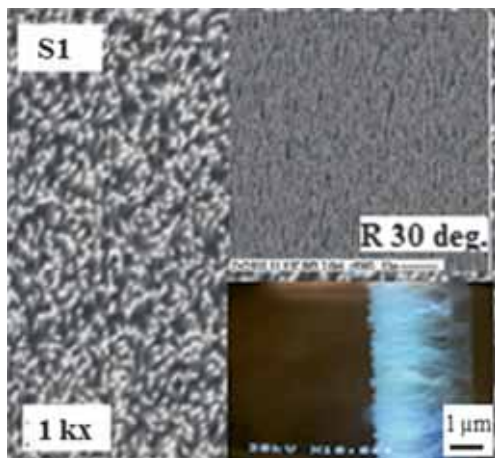


Figure 9. SEM images of ZnO NWs growth on ITO-glass/60 min, Ar/O₂ = 300/40 sccm, at 550°C (inset shows film tilted at 30°).

time had a greater influence on the length of NW than the diameter.

3.4 Growth of ZnO NWs as a function of O₂ rate flow variation

The fourth group of investigation was to study the effect of O₂ gas flow rates variation on the length and morphology of the synthesized ZnO NWs. These experiments were conducted by varying the O₂ flow rate of 40, 50 and 60 sccm under the following fixed conditions: argon gas flow rate of 300 sccm, furnace temperatures of TC = 900°C and TR = 550°C for 60 min reaction time, and final growth pressure of 100 Torr. Figures 9, 10, and 11 show fine NWs synthesized under gas flow rates ratio of 300/40, 300/50 and 300/60, respectively. It can be seen that high-density NWs have been produced. The typical NWs appear to grow straight and VA on the ITO-glass substrate coated with ZnO seed layer, as demonstrated in figure 10.

Figure 12 shows collection data for comparison of SEM cross-sections of as-synthesized ZnO NWs on ITO-glass under constant argon gas flow rate of (300 sccm), with various oxygen gas flow rates of 40, 50 and 60 sccm. Global data for average length of ZnO NWs grown on ITO-glass via CVD technique at a certain growth parameter were drawn as a histogram shown in figure 13. Typical wires length around 10 μm at 50 sccm rate flow of oxygen gas and constant argon rate flow of 300 sccm can be observed. This is considered as optimum values achieved in the present investigations. It was found that the wire length is very sensitive to the flow rate of oxygen in the growth system.

3.5 Typical structure and morphology analysis of ZnO NWs

X-ray diffraction (XRD) was employed to investigate the crystal structure of the ZnO NWs. Figure 14 shows

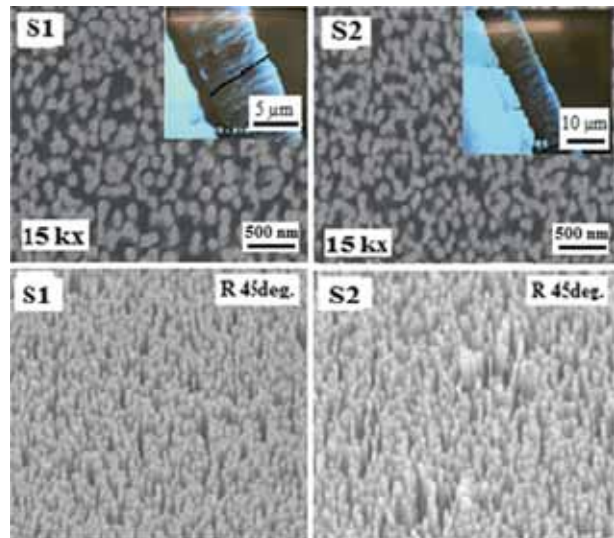


Figure 10. Typical SEM images of ZnO NWs on ITO-glass grown at 60 min. Ar/O₂ = 300/50 sccm, average diameters: S1 = 95, S2 = 70 nm.

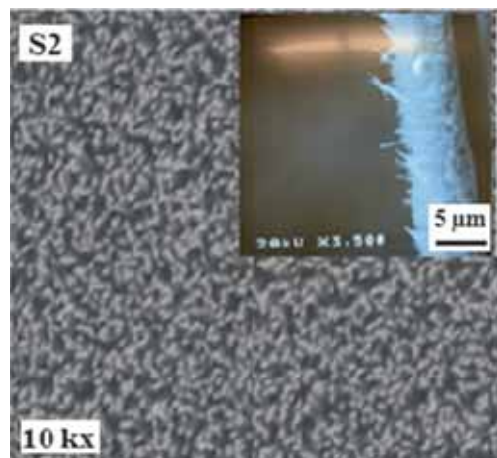


Figure 11. SEM image of ZnO NWs grown on ITO-glass/60 min, 15 mM, Zn = 4 g (inset shows cross-section = 7 μm).

typical XRD patterns of ZnO NWs on ITO-glass as synthesized via CVD method. It was found that only one strong ZnO (0 0 2) diffraction peak with small line width was observed in the spectrum. This diffraction peak at $2\theta = 34.93^\circ$ can be easily assigned to a ZnO hexagonal wurtzite structure. The XRD peak is slightly shifted to higher angle for ZnO (002). This shift could be due to small strain generation in the materials structure during synthesis. There is no peak from other impurities, such as Zn metal that are detected in the patterns, indicating that the product is formed with high purity.

Transmission electron microscopy (TEM) was employed to characterize the as-synthesized ZnO NWs. Very small amount of this product was scraped from the ITO top surface. These ZnO NWs were prepared on 3.05 mm formvar-coated copper grid. The TEM image in figure 15a and b shows the

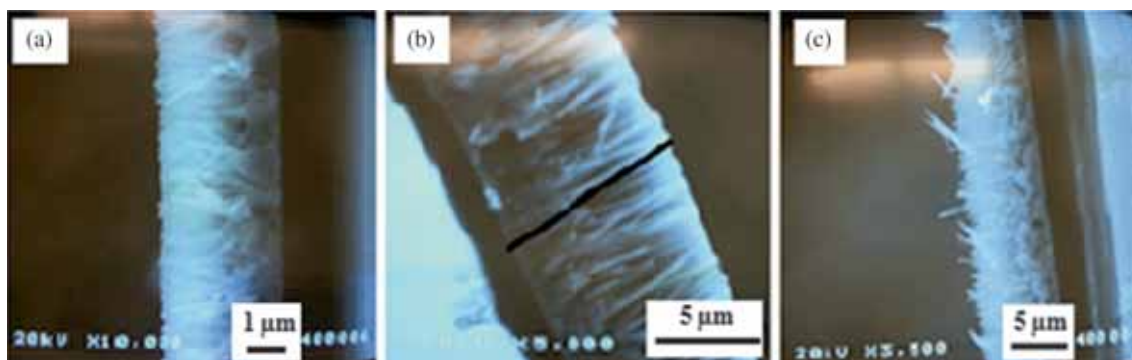


Figure 12. Summarized cross-sections of ZnO NWs grown on ITO with wire lengths of (a) 3, (b) 10 and (c) 7 μm at constant argon flow rates of 300 sccm and various O_2 flow rates of 40, 50 and 60 sccm, respectively.

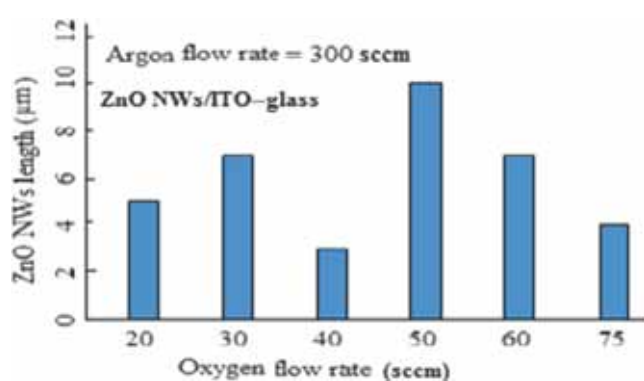


Figure 13. Histogram of average length of ZnO NWs vs. oxygen gas flow rate. At fixed argon flow rate of 300 sccm and 60 min growth time.

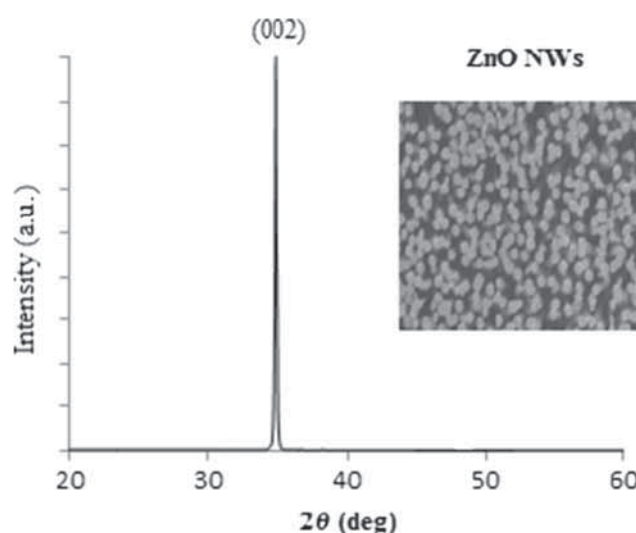


Figure 14. XRD of typical ZnO NWs on ITO-glass as synthesized via CVD method.

clusters and individual ZnO NWs, respectively. TEM images also show that the diameter size is varied significantly along the wire length. The measured diameters of ZnO NWs are 100 and 150 nm for top and bottom, respectively. Figure 15c shows an EDX spectrum of the ZnO NWs. Features of Zn and O atoms can be observed in this spectrum. The appearance of Cu peak in the spectrum is due to the TEM copper grid. The EDX detection of just Zn and O atoms confirms the high purity of the prepared ZnO.

Figure 16 demonstrates the high quality of the as-synthesized ZnO NWs arrays grow with a c -axis orientation perpendicular to the substrate. Typical SEM image of ZnO NWs is shown in figure 16a. The single ZnO NWs and its related selected area electron diffraction pattern is shown in figure 16b. It is suggested that the ZnO NWs shows the excellent preferred (002) reflection. This is previously confirmed by XRD analysis, as shown in figure 14.

ZnO NWs can be synthesized with a growth time from 20 to 60 min, and the length of NWs is mainly determined by the growth time. The longest NWs have average length of around 10 μm and average diameter of 100 nm. ZnO NWs cannot be formed unless the growth temperature at the precursor is 900°C. The ZnO NWs made in this method are VA, and have small wire diameter, long length and high density,

which are suitable for building hybrid metal oxide/organic solar cells on ITO- and FTO-coated glass substrates as the substrate temperatures are equal to 550°C.

3.6 Growth model and mechanism of VA ZnO NWs/NRs

ZnO has the wurtzite structure, as shown in figure 17a, which has a hexagonal unit cell with space group $C6mc$ and lattice parameters $a = 0.396$ and $c = 0.52065$ nm. The oxygen anions and Zn cations form a tetrahedral unit. The entire structure lacks central symmetry. Figure 17a shows the ZnO crystal, which consists of an alternating sequence of hexagonally closed-packed layers of Zn^{2+} and O^{2-} ions along the c -direction. The ZnO {0001} faces have the highest energy and low index planes. The growth model of VA ZnO NWs on ITO-glass substrate depends on the texture of ZnO seed layer, zero lattice mismatch between ZnO nanoparticles as a seed layer and the ZnONWs grown. VA ZnO NWs or NRs can be synthesized by heteroepitaxy or homoepitaxy growth.

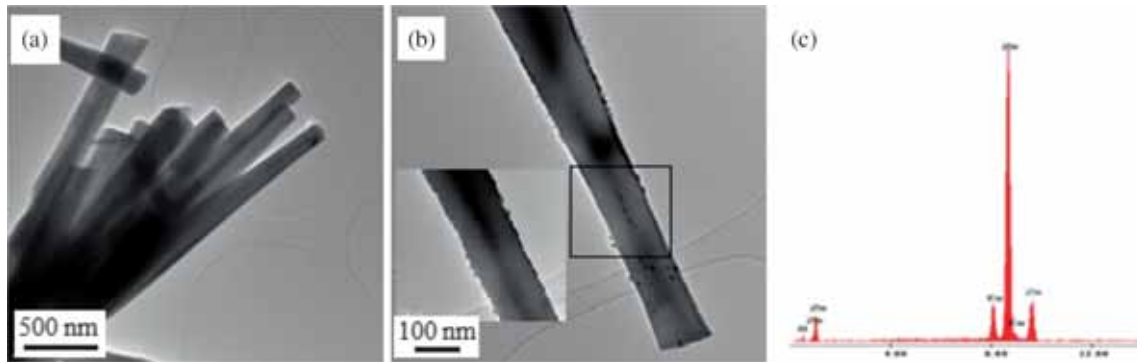


Figure 15. TEM images of (a) clusters of ZnO NWs, (b) single ZnO NWs, and the inset shows magnified image. (c) EDX spectrum measured for ZnO nanowires.

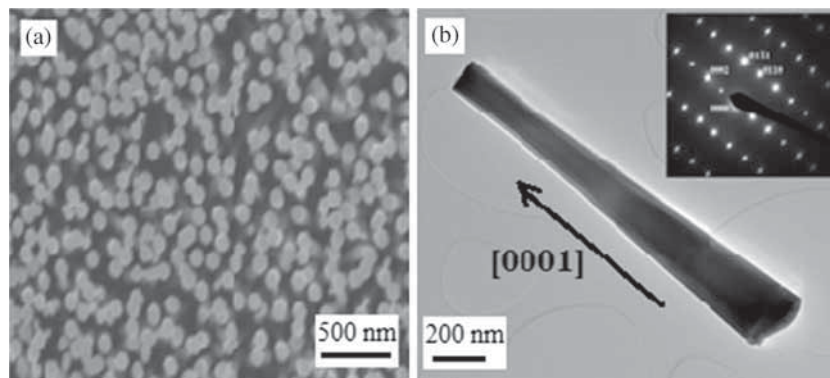


Figure 16. (a) SEM—top view image of typical ZnO NWs and (b) TEM images of single-crystalline ZnO NWs (inset is the corresponding SAED pattern of the ZnO NWs).

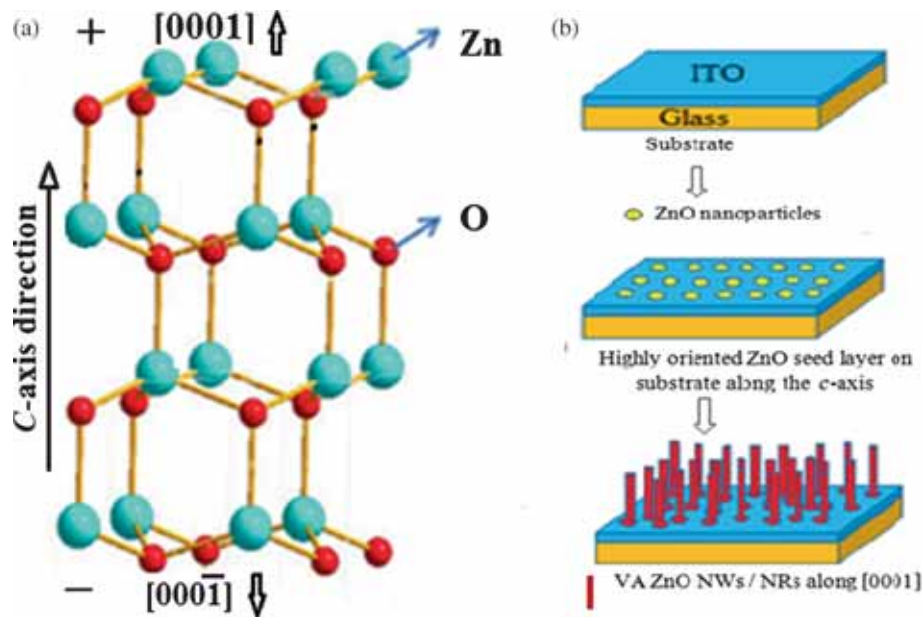


Figure 17. (a) Wurtzite crystal structure model of ZnO and (b) ZnO NWs growth mechanism process.

In heteroepitaxy growth, substrates with a small lattice mismatch between ZnO NWs are needed to provide a good template for VA ZnO NWs. In the present work, homoepitaxy growth with highly (0002) oriented ZnO seeds layer facilitate the aligned growth of ZnO NWs. It is well known that ZnO wetting layer formed prior to NWs/NRs growth has been reported by many authors [33,34]. Figure 17b demonstrates the growth process of ZnO NWs on ZnO seed layer.

4. Conclusions

In this study, ZnO NWs were synthesized on ITO-coated glass substrate by a CVD technique. The formation of the VA ZnO NWs was supported by ZnO seeding layer on the ITO substrate at growth temperature of 550°C under argon and oxygen gases flows. The CVD parameters variation results in a typical and optimized parameters of ZnO NWs growth of VA, long, high density and small diameters. These were mainly analysed with SEM and XRD for the synthesized ZnO NWs by CVD method. The XRD and energy-dispersive X-ray spectroscopy analyses for typical sample clearly indicates that well-ordered single crystal along the *c*-axis with highly pure ZnO NWs are formed. The TEM analysis confirmed the XRD results. It was found that in typical conditions the measured length of these NWs was around 10 µm, while the diameters were in between 50 and 100 nm. The growth model confirmed the epitaxial growth of VS mechanism. The benefit of this technique is to produce high-quality, long and VA ZnO NWs, which can be applied on the electrode of dye-synthesized solar cell application.

Acknowledgements

We would like to acknowledge the financial support via the Department of State/USA/CRDF/ISFP and the opportunity afforded by the University of Technology, Baghdad, Iraq. We also thank Dr W Zhou and his group at AMIRI/University of New Orleans/Louisiana and for the benefit of using their materials and equipment, and for giving us the useful suggestions for research.

References

- [1] Liu B and Zeng H C 2003 *J. Am. Chem. Soc.* **125** 4430
- [2] Ibupoto Z H, Khun K, Eriksson M, AlSalhi M, Atif M, Ansari A and Willander M 2013 *Materials* **6** 3584
- [3] Foo K L, Hashim U, Muhammad K and Voon C H 2014 *Nanoscale Res. Lett.* **9** 429
- [4] Lu L, Chen J, Li L and Wang W 2012 *Nanoscale Res. Lett.* **7** 293
- [5] Hsiao C-C and Luo L-S 2014 *Sensors* **14** 12219
- [6] Zhang Q, Dandeneau S C, Zhou X and Cao G 2009 *Adv. Mater.* **21** 4087
- [7] Yang W, Wan F, Chen S and Jiang C 2009 *Nanoscale Res. Lett.* **4** 1486
- [8] Ramachandran K, Kumar G G, Kim A R and Yoo D J 2014 *Bull. Korean Chem. Soc.* **35** 1091
- [9] Elamin N and Elsanousi A 2013 *J. Appl. Ind. Sci.* **1** 32
- [10] Rashidi H, Ahmadpour A, Bamoharram F F, Zebarjad S M, Heravi M M and Tayari F 2014 *Chemical Papers* **68** 516
- [11] Zak A B, Majid W H A, Wang H Z, Yousefi R, Golsheikh A M and Ren Z F 2013 *Ultrason. Sonochem.* **20** 395
- [12] Nayak A P, Katzenmeyer A and Gosho Y 2010 *Proceedings of the national conference on undergraduate research (NCUR)*, University of Montana, Missoula, April 15–17
- [13] Sornalatha D J and Murugakoothan P 2013 *J. Emerg. Technol. Adv. Eng.* **3** 414
- [14] Khan Z R, Khan M S, Zulfequar M and Khan M S 2011 *Mater. Sci. Appl.* **2** 340
- [15] Foo K L, Uda Hashim, Kashif Muhammad and Chun Hong Voon 2014 *Nanoscale Res. Lett.* **9** 429
- [16] Prakash T, Jayaprakash R, Neri G and Kumar S 2013 *J. Nanomater.* **2013** 8
- [17] Lu L, Chen J, Li L and Wang W 2012 *Nanoscale Res. Lett.* **7** 293
- [18] Rodwihok C, Gardchareon A, Phadungthitidhada S, Wongratanaphisan D and Choopun S 2014 *Thai J. Phys. Series* **10** 25001
- [19] Hassan N K, Hashim M R, Mahdi M A and Allam N K 2012 *ECS J. Solid State Sci. Technol.* **1** 86
- [20] Ma T, Wang Y, Tang R, Yu H and Jiang H 2013 *J. Appl. Phys.* **113** 204503
- [21] Dongshan Y, Tarek T, James T M J, Valentin C and Curtis R T 2010 *Nanoscale Res. Lett.* **5** 1333
- [22] Giri P K, Patel P K, Panchal C J *et al* 2007 *Synth. React. Inorg. Metal-Org. Nano-Metal. Chem.* **37** 437
- [23] Khanlary M R, Vahedi V and Reyhani A 2012 *Molecules* **17** 5021
- [24] Greene L E, Yuhua B D, Law M, Zitoun D and Yang P 2014 *Inorg. Chem.* **45** 7535
- [25] Kim K H, Utashiro K, Abe Y and Kawamura M 2014 *Int. J. Electrochem. Sci.* **9** 2080
- [26] Kumar P S, Yogeshwari M, Raj A D, Mangalaraj D, Nataraj D and Pal U 2009 *J. Nano Res.* **5** 223
- [27] Lucas M, Wang Z L and Riedo E 2010 *Phys. Rev. B* **81** 045415
- [28] Zhang N, Yi R, Shi R, Gao G, Chen G and Liu X 2009 *Mater. Lett.* **63** 496
- [29] Yong-Zhe Z, Li-Hui W, Yan-Ping L, Er-Qing X, De Y and Jiang-Tao C 2009 *Chin. Phys. Lett.* **26** 038201
- [30] Hughes W L and Wanga Z L 2005 *Appl. Phys. Lett.* **86** 043106
- [31] Gui Z, Liu J, Wang Z, Song L, Hu Y, Fan W and Chen D 2005 *J. Phys. Chem. B* **109** 1113
- [32] Wua C-Y, Hsua H-C, Chenga H-M, Yanga S and Hsieha W-F 2006 *J. Cryst. Growth* **287** 189
- [33] Tasker P W 1979 *J. Phys. C: Solid State Phys.* **12** 4977
- [34] Greene L E, Law M, Tan D H, Montano Ma, Goldberge J, Gomorja G and Yang P 2005 *Nano Lett.* **5** 1231